Nonlinear-Linear Analysis of Microwave Mixer with Any Number of Diodes

MAREK T. FABER AND WOJCIECH K. GWAREK

***Abstract*—A theory is presented for analyzing mixers with any number of diodes. Both the nonlinear and linear steps of the analysis are included. The diodes are characterized by both nonlinear conductance and nonlinear capacitance. Any linear embedding network is allowed. It is assumed that both the parameters of the linear part of a mixer circuit and the parameters of the diodes are known. This general approach to microwave circuits with diodes, which is a qualitatively new problem in circuits analysis, allows to investigate any diode mixer with deep insight into its operation. A computer program has been developed to perform the analysis and all computations. The program has been utilized to analyze a crossbar mixer configuration which exhibits extremely encouraging performance. Some computed results are presented herein.**

I. Introduction

MICROWAVE mixer analysis has been an important problem for more than thirty years, and is still an evolving art. Starting from the fundamental work of Torrey and Whitmer [1] and up to the late sixties [2], [3] very simplified mixer models were analyzed. The computer era has opened the possibility of more accurate computer-aided analyses based on less simplified mixer models. It was the first basic problem to analyze a single-diode mixer without the assumptions of sinusoidal drive, linearity of the diode capacitance, and short- or open-circuit terminals seen by the diode at pump (LO) harmonics and various mixing products. Egami [4], Gwarek [5], [6], Kerr [7], and Held [8] have contributed to the problems solution and satisfactory practical results have been reported by Held and Kerr [9].

No theory has been still available for accurate analysis of multidiode mixers and such mixers have been analyzed in very simplified ways and their development has mainly been empirical. However, it is possible to generalize the aforementioned one-diode mixer analyses to the multidiode case. A generalization to subharmonically pumped and balanced two-diode mixers has been recently reported [10].

In this paper a method for analyzing a mixer with any number of diodes is presented. The diodes and the circuit models used in the analysis are similar to those used in the one-diode mixer analyses. No extra simplifying assumptions are taken.

Let us consider a mixer with M diodes. Its model is shown on Fig. 1. A linear time-invariant network (LTIN) possesses $M+3$ ports.[1] Each of the ports $1,2,\cdots,M$ is loaded with parallel connection of a nonlinear conductance and a nonlinear capacitance representing the junction of the respective diode. All other elements of the equivalent circuits of the diodes (including series resistances, package capacitances, whiskers inductances, and so on) are included in the LTIN. Port numbered $M+1$ is connected to the pump (LO) source. Ports $M+2$ and $M+3$ are signal input and output, respectively.

In practical circuits the level of the pumping signal is much higher than that of the input signal. This allows to divide the analysis into two steps [1], [2], [3]. In the first step, called *nonlinear analysis*, the signal source is not taken into account and the goal of this step is to find the waveforms of voltages $u_{jm}(t)$, $m=1,2,\cdots,M$, due to the driving from the pump source $E_p e^{j\omega_p t}$, where ω_p is the pump frequency. The functions $g_m(u_{jm})$ and $c_m(u_{jm})$ are known, thus determination of the waveforms u_{jm} allows to find the dependences $g_m(t)$ and $c_m(t)$. From this point on in the analysis, the pump source may be ignored, and the circuit can be treated as a circuit with parametric elements $g_m(t)$, $c_m(t)$ periodically varying with time. Such a circuit can be described by a set of linear equations, and the mixer performance can be determined. This is the task of the *linear* step of the mixer *analysis*.

II. Nonlinear Analysis

The method of nonlinear analysis presented here arises from previously published methods of one-diode mixer analysis, namely correction sources method [5] and reflecting waves method [7]. It was found [6] that in their advanced forms both lead to the same computer algorithm. The latter method is superior by the cleարity of physical interpretation of the employed iteration process.

The aim of the nonlinear analysis is to find the waveforms $u_{jm}(t)$ on the diodes' junctions. Since the input signal has a much smaller level than the pumping signal, the mixer circuit is, for the purpose of the nonlinear analysis, reduced to that of Fig. 2. A linear time-invariant network LTIN2 has been formed from the LTIN of Fig. 1 by loading the ports $M+2$ and $M+3$ with the impedance

Manuscript received March 28, 1980; revised July 24, 1980.

M. T. Faber is with the Institute of Electronics Fundamentals, Technical University of Warsaw, Nowowiejska 15/19, 00-665 Warszawa, Poland.

W. K. Gwarek is with the Institute of Radioelectronics, Technical University of Warsaw, Nowowiejska 15/19, 00-665 Warszawa, Poland.

[1] If the diodes are dc biased, one or more extra ports have to be added for connecting the biasing sources. Since this is not a typical case for microwave mixer, the dc sources will not be considered here. The discussion presented in the paper can be easily extended to the case when the dc bias is present.

0018-9480/80/1100-1174$00.75 ©1980 IEEE

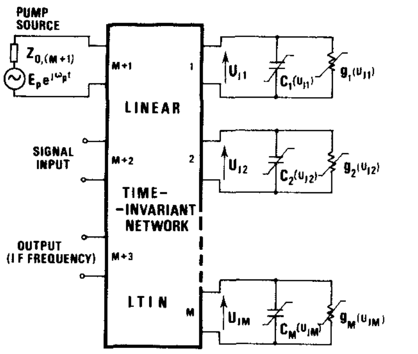

Fig. 1. General equivalent circuit of a mixer with M diodes.

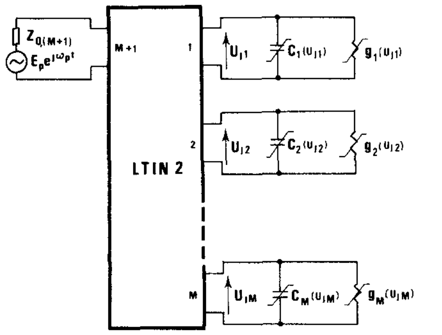

Fig. 2. Mixer model used in the nonlinear analysis.

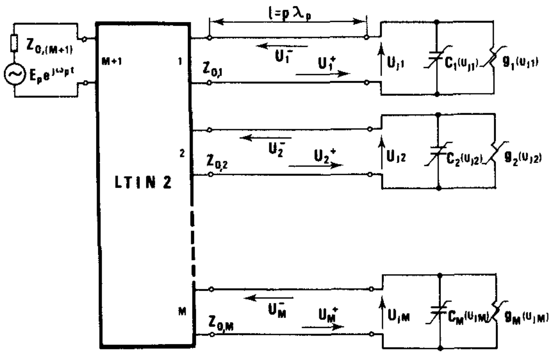

Fig. 3. Mixer model with long transmission lines inserted between the diodes' junctions and the rest of the circuit.

of a signal generator and the input impedance of an intermediate frequency amplifier, respectively. In the method it is generally assumed that the parameters of LTIN2 are known for relevant frequencies. Let us assume that the circuit will be described by the elements of the S matrix defined with the loading impedances Z_{om} at the respective ports.

The idea of the method is to change the circuit of Fig. 2 in a way that the new circuit has the same steady-state but in which this steady-state can be determined easier.[2] Satisfactory results are obtained by changing the circuit of Fig. 2 to that of Fig. 3. Dispersionless lossless transmis-

[2]It is assumed that there is only one steady-state in the circuit. In the circuit of Fig. 2 containing nonlinear reactances there is a theoretical possibility of existing more than one steady-state for a particular pumping. However operation with two (or more) possible steady-states, if achieved, would cause instability of the mixer parameters. That kind of operation should not occur in a properly designed mixer and is not considered here.

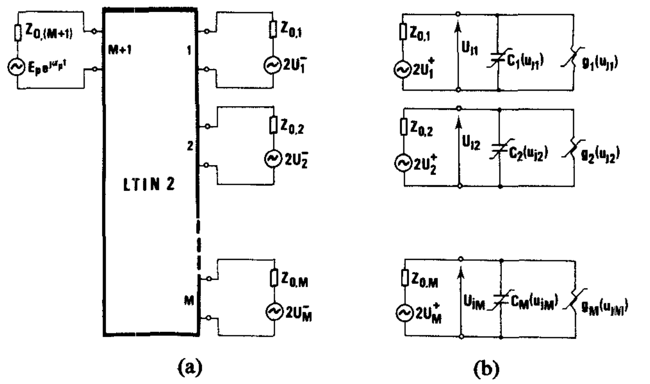

Fig. 4. Separation of the diodes from the rest of the circuit employing the concept of incident and reflected waves.

sion lines inserted between the junctions' nodes and respective ports of LTIN2 have the lengths

$$l = p \cdot \lambda_p$$

where λ_p is the wavelength for the pump angular frequency ω_p, and p is the large integer. For the steady-state those transmission lines are "transparent" for the pump frequency, any of its harmonics and for dc signals.

Let us investigate the circuit of Fig. 3 in the time following connection of the source E_p to the port number $M+1$ of LTIN2. If the transmission lines in the circuit are sufficiently long (p is large) the circuit LTIN2 will reach the local steady-state with the right-hand side propagating waves u_m^+

$$u_m^+(t) = \sum_{k=-\infty}^{\infty} U_{mk}^+ e^{jk\omega_p t} \tag{1a}$$

where $m = 1, 2, \cdots, M$.

Before the reflected waves return from the diodes, the LTIN2 circuit sees, on ports $1, 2, \cdots, M$, only the characteristic impedances of the lines. Since the circuit is driven sinusoidally initially only the terms of the frequency ω_p are present in the sum of (1). Thus

$$U_{mk}^+ = \frac{1}{2} E_p S_{m,M+1}(k\omega_p) \sqrt{\frac{Z_{om}}{Z_{o,M+1}}}, \qquad \text{for } |k| = 1$$

$$U_{mk}^+ = 0, \qquad \text{for } |k| \neq 1$$

and therefore

$$u_m^+(t) = \frac{1}{2} \operatorname{Re}\left[E_p S_{m,M+1}(\omega_p) \sqrt{\frac{Z_{om}}{Z_{o,M+1}}}\, e^{j\omega_p t} \right]. \tag{1b}$$

When the propagating waves reach the ends of the lines loaded with the diodes they become sources of the electromotive forces

$$e_m^+(t) = 2u_m^+(t)$$

with the internal impedances Z_{om}. At that moment this causes the waveforms of voltage u_{jm} at the mth diode junction to be calculated from the differential equation (2) describing the relations in the diodes' circuits shown in Fig. 4(b)

$$\frac{du_{jm}(t)}{dt}=\frac{2u_m^+(t)-u_{jm}(t)\left[1+g_m(u_{jm})Z_{om}\right]}{Z_{om}c_m(u_{jm})}. \quad (2)$$

Equation (2) can be solved by one of the numerical integration methods. As a result, the junction voltage and current waveforms are obtained

$$u_{jm}(t)=\sum_{k=-\infty}^{\infty} U_{jmk}\,e^{jk\omega_p t} \quad (3)$$

$$i_{jm}(t)=\sum_{k=-\infty}^{\infty} I_{jmk}\,e^{jk\omega_p t}=\frac{2u_m^+(t)-u_{jm}(t)}{Z_{om}}. \quad (4)$$

The voltages and currents calculated above represent the local steady-state at the diodes junctions reached after arrival of the waves u_m^+. When that state is reached, the left-hand side waves u_m^- are propagating towards the LTIN2 circuit. The waves u_m^- are those reflected from the diodes upon incidence of the waves u_m^+ and can be expressed as

$$u_m^-(t)=\sum_{k=-\infty}^{\infty} U_{mk}^-\,e^{jk\omega_p t}=\sum_{k=-\infty}^{\infty} U_{mk}^+\Gamma_{mk}\,e^{jk\omega_p t}$$
$$=\sum_{k=-\infty}^{\infty} U_{mk}^+\frac{Z_{jmk}-Z_{om}}{Z_{jmk}+Z_{om}}\,e^{jk\omega_p t} \quad (5)$$

where $Z_{jmk}=U_{jmk}/I_{jmk}$.

Formula (5) needs to be modified for practical purposes since in a nonlinear circuit it may happen that $U_{mk}^+=0$ and $\Gamma_{mk}=\infty$[3] which is unacceptable for a computer. Let us notice that in the circuit of Fig. 4(b)

$$u_m^+(t)=\frac{1}{2}\left[u_{jm}(t)+Z_{om}i_{jm}(t)\right]. \quad (6)$$

Thus (5) can be transformed to the form

$$u_m^-(t)=\frac{1}{2}\sum_{k=-\infty}^{\infty}(Z_{jmk}-Z_{om})I_{jmk}\,e^{jk\omega_p t}. \quad (7)$$

After some amount of time the waves u_m^- reach the ports of LTIN2. The wave u_m^- incident on port m is interpreted as a source of electromotive force $e_m^-=2u_m^-$ and internal impedance Z_{om} as shown on Fig. 4(a). The wave is partially reflected from the port of entry and partially passes through the LTIN2 to the other ports. The new local steady-state in LTIN2 is achieved and new right hand side waves described by formula (8) start travelling towards the diodes

$$u_m^{+\prime}(t)=\sum_{k=-\infty}^{\infty}\left[\sum_{p=1}^{M} U_{pk}^- S_{mp}(k\omega_p)\sqrt{\frac{Z_{om}}{Z_{op}}}\right]e^{jk\omega_p t}. \quad (8)$$

The process of calculating sequential values of u_m^+ resulting from reflections in the transmission lines can be treated as an iteration process convergent to the value describing the steady-state of the all circuit. Formula (1) gives the initial value of u_m^+ in this process; formulas (2), (7), (8) show how to calculate the next step of iteration when the former step has been calculated.

Several of the presented equations contain sums with index k varying from minus to plus infinity which corresponds to investigation of infinite number of harmonics. In practical calculations, the number of these harmonics has to be reduced to finite value $K(-K\leqslant k\leqslant K)$. Eventual waveforms of the voltages $u_{jm}(t)$ are obtained by solving (2). Deletion of the components of $u_m^+(t)$ for $|k|>K$ is equivalent to the assumption that the impedance Z_{om} is seen by the mth diode at harmonics higher than K. The choice of K depends on the circuit under investigation, required accuracy of the calculations, and restrictions on the time of computations. It usually varies from three to seven.

[3]It actually happens for the first reflection from the diodes because $U_{mk}^+=0$ for $|k|\neq 1$ while in general $U_{mk}^-\neq 0$.

III. Linear Analysis

In the nonlinear step of the mixer analysis the LO waveforms $u_{jm}(t)$ at each of the M diode junctions have been determined. Since the voltages $u_{jm}(t)$ are time periodic functions, then $g_m(t)$ and $c_m(t)$ are also periodic with the same period. These functions may be expanded into Fourier series

$$g_m(t)=\sum_{l=-\infty}^{\infty} G_{m,l}\exp(jl\omega_p t), \qquad G_{m,l}=G_{m,-l}^* \quad (9)$$

$$c_m(t)=\sum_{l=-\infty}^{\infty} C_{m,l}\exp(jl\omega_p t), \qquad C_{m,l}=C_{m,-l}^* \quad (10)$$

where $m=1,2,\cdots,M$, and M is the number of diodes. At this point of the analysis the LO source may be excluded from further investigation and the small-signal currents $i_m(t)$ and voltages $u_m(t)$ resulting from the mixing process can be taken into consideration. For each diode the frequency components of $i_m(t)$ and $u_m(t)$ are interrelated by the *conversion matrix of the diode* [1], [5], [6], [9]. The subscript notation for the sideband quantities follows that of Saleh [2], e.g., subscript l indicates frequency $\omega_l=\omega_0+l\omega_p$. For the mth diode the conversion matrix Y_m is a square matrix with the elements given by

$$Y_{m,l,n}=G_{m,l-n}+j(\omega_0+l\omega_p)C_{m,l-n} \quad (11)$$

where the subscript m indicates the diode while the subscripts l and n indicate the row and the column in the matrix Y_m. $G_{m,k}$ and $C_{m,k}$ are the Fourier coefficients of the mth diode conductance and capacitance at the frequency $\omega_k=k\omega_p$ as defined in (9) and (10). If only L components of the small-signal currents and voltages are considered each of the conversion matrices Y_m has the size $(2L+1)\times(2L+1)$.

Having determined all the Y_m matrices of all the M diodes, the *admittance conversion matrix Y_C of the whole mixer* can be composed. The mixer may be represented as a multifrequency linear multiport network. Since the time-invariant part of the mixer circuit is linear, the diodes and external load admittances are interconnected at each frequency ω_l by $M+1$ port networks. Load admittances at frequencies other than signal, image, and IF may be included into respective multiport networks. For example,

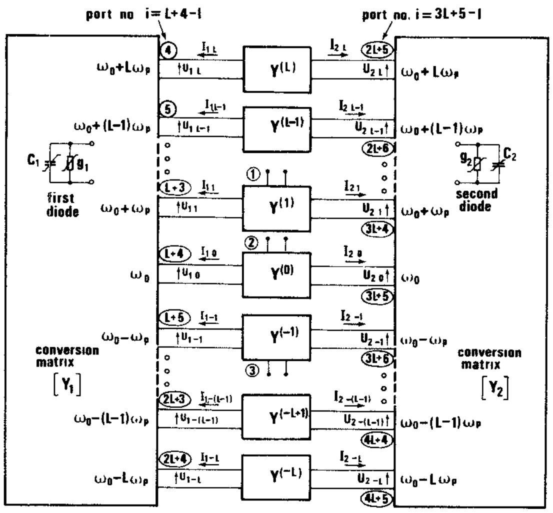

Fig. 5. Small-signal representation of a two-diode mixer as a multiport network. Frequency ω_l at diodes' ports $i=L+4-l$ and $i=3L+5-l$, i.e. $I_{L+4-l}=I_{1,l}$; $U_{L+4-l}=U_{1,l}$; $I_{3L+5-l}=I_{2,l}$; $U_{3L+5-l}=U_{2,l}$. Usually input at frequency ω_1 or ω_{-1} (port 1 or 3), output at intermediate frequency ω_0 (port 2).

if we consider a mixer having input, output, and image signals at frequencies ω_1, ω_0, ω_{-1}, respectively, the $M+1$ port networks at frequencies ω_l, $l \neq -1,0,1$, may be reduced to M port networks. This is pictured in Fig. 5 for the case $M=2$.

It is necessary to determine $Y^{(l)}$ matrices describing the time-invariant part of the mixer at frequencies $\omega_l = \omega_0 + l\omega_p$ $(-L \leqslant l \leqslant L)$. Since $Y_{i,j}(-\omega)=Y^*_{i,j}(\omega)$, the Y parameters may be determined at frequencies ω_0, $l\omega_p+\omega_0$ and $l\omega_p-\omega_0$, $l=1,2,\cdots,L$ (e.g., computed or by measurements of the S parameters) and then the $Y^{(l)}$ matrices can be computed.

Let us introduce the quantities

$$\begin{aligned} i_0 &= 2 \\ i_1 &= L+4 \\ i_2 &= 3L+5 \\ i_3 &= 5L+6 \\ &\vdots \\ i_m &= L(2m-1)+m+3 \\ &\vdots \\ i_M &= L(2M-1)+M+3 \end{aligned} \tag{12}$$

and let us number the ports in the way as it was done in Fig. 5 for the two-diode mixer, i.e.,

$$\begin{aligned} i &= i_1 - l, && \text{for the first diode} \\ i &= i_2 - l, && \text{for the second diode} \\ &\vdots \\ i &= i_m - l, && \text{for the } m\text{th diode} \\ &\vdots \\ i &= i_M - l, && \text{for the last } M\text{th diode,} \\ &\text{where} && -L \leqslant l \leqslant L \end{aligned}$$

and

$$i = i_0 - l, \qquad \text{for the mixer input and output, where } l=-1,0,1.$$

It is convenient to express the conversion matrix of the mixer Y_C by means of matrices Y_D and Y_S

$$Y_C = Y_D + Y_S.$$

The matrix Y_D is composed of the matrices Y_m of the diodes and its nonzero elements are

$$Y_{D_{i_m-l,\, i_m-n}} = Y_{m,l,n} \tag{13}$$

where $m=1,2,\cdots,M$; $l=-L,\cdots,-1,0,1,\cdots,L$; $n=-L,\cdots,-1,0,1,\cdots,L$ and $Y_{m,l,n}$ and i_m are given by (11) and (12), respectively.

The matrix Y_S is composed of the matrices $Y^{(l)}$ of the time-invariant part of the mixer circuit. Its nonzero elements are

$$Y_{S_{i_p-l,\, i_r-l}} = Y^{(l)}_{p,r}, \qquad \text{for } l=-L,\cdots,-2,2,\cdots,L$$

$$Y_{S_{i_t-l,\, i_w-l}} = Y^{(l)}_{t+1,w+1}, \qquad \text{for } l=-1,0,1 \tag{14}$$

where $p=1,2,\cdots,m,\cdots,M$; $r=1,2,\cdots,m,\cdots,M$; $t=0,1,2,\cdots,m,\cdots,M$; $w=0,1,2,\cdots,m,\cdots,M$; and $i_0, i_1, i_2, \cdots, i_m, \cdots, i_M$ are defined in (12). The matrices Y_D and Y_S are pictured on Figs. 6 and 7 for the case of two-diode mixer ($M=2$).

The conversion matrix Y_C of the mixer is a *sparse square matrix* having the size $(2LM+M+3)\times(2LM+M+3)$. Its *density factor d* depends on L and M

$$d = \frac{M+1}{2LM+M+3} + \frac{2M(2L^2+1)}{(2LM+M+3)^2}. \tag{15}$$

When the matrix Y_C is determined, the *impedance matrix of the mixer* can be found

$$Z_C = (Y_C)^{-1}$$

and the three-frequency mixer model having ports associated with the signal, image, and intermediate frequencies may be used to determine all the small-signal properties of the mixer [11]. The stability problems and matching conditions can be investigated.

As far as the noise properties of the mixer are concerned, it should be noted that *the noise produced by one diode is not correlated with the noise of any other diode.* Thus for each of the diodes, the *shot noise* correlation matrices can be found in the way described by Held and Kerr [9] for a one-diode mixer. *Thermal noise* generated in the time-invariant part of the mixer can be described by the correlation matrix as it has been done by Twiss [12]. The noise correlation matrix of the whole mixer can be composed in the way described above in this paper. Then the noise properties of the mixer (the equivalent input noise temperature or the noise figure) can be determined. Noise analysis, however, will not be dealt with in this paper.[4]

[4]This will be done in a paper to be published shortly.

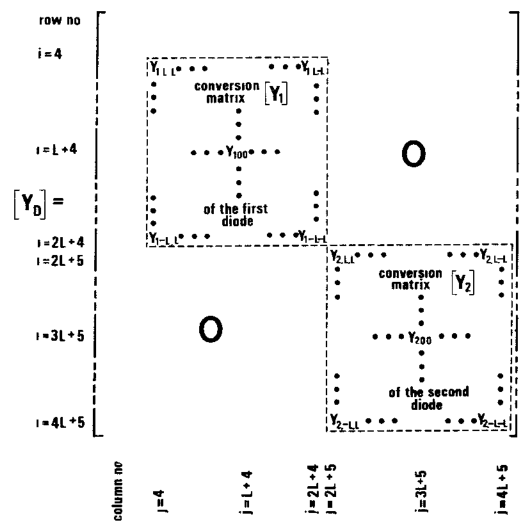

Fig. 6. Matrix Y_D in the case of a two-diode mixer ($M=2$). The elements of the conversion matrix Y_1 of the first diode are in rows from $i=4$ to $i=2L+4$ and columns from $j=4$ to $j=2L+4$. The elements of the conversion matrix Y_2 of the second diode are in rows from $i=2L+5$ to $i=4L+5$ and columns from $j=2L+5$ to $j=4L+5$. The nonzero elements of the matrix Y_D are given in (13) if $M=2$.

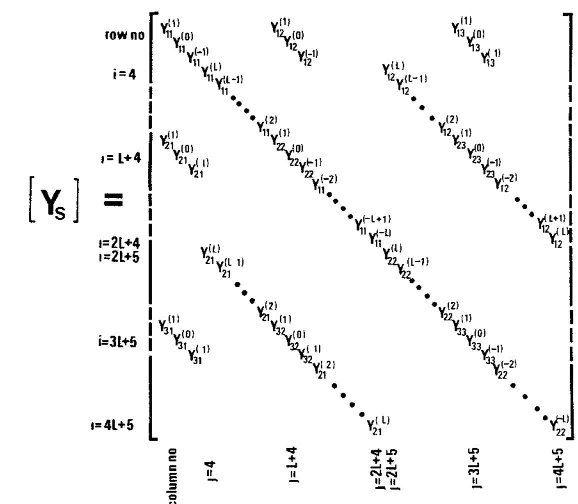

Fig. 7. Matrix Y_S in the case of a two-diode mixer ($M=2$). The matrix Y_S is composed of the elements of the $Y^{(l)}$ matrices. The nonzero elements of the matrix Y_S are given in (14) if $M=2$.

IV. Computer Implementation of the Theory

A computer has to be employed for practical application of the above theory. Therefore, a computer program written in Fortran has been developed to perform the analysis and all the computations. The program allows the study of the influence of the diode parameters on mixer performance as well as effects of loads at the pump frequency, its harmonics, signal, image, and idle frequencies. Frequency and thermal dependences of mixer parameters can be investigated. Each diode may have different parameters, thus unbalance effects due to the diodes and the embedding network can be studied. The program has been utilized to analyze microwave mixers with two Schottky diodes.

We have found that in most practical cases, it is sufficient to consider 4 to 6 harmonics in the nonlinear step and 6 to 8 harmonics in the linear step of the mixer analysis. It should be noted that in the nonlinear analysis, deletion of the higher harmonics has the physical interpretation equivalent to the assumption that the characteristic impedances Z_{om} of the transmission lines are seen by the diodes at the deleted harmonics. In the linear analysis, such a physical interpretation does not exist. One run of the program takes approximately 1 min on CDC CYBER 73 computer, if standard procedures for numerical integration and inversing of complex matrices are called from the computer library. It can be speeded up by utilizing procedures written specially for these particular applications. It looks profitable to utilize a sparse matrix technique when analyzing mixers with more than two diodes.

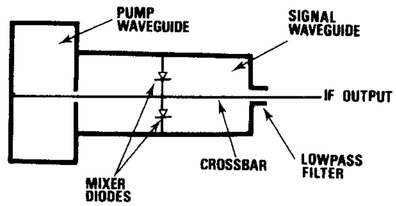

Fig. 8. Schematic diagram of the crossbar mixer (transverse cross section).

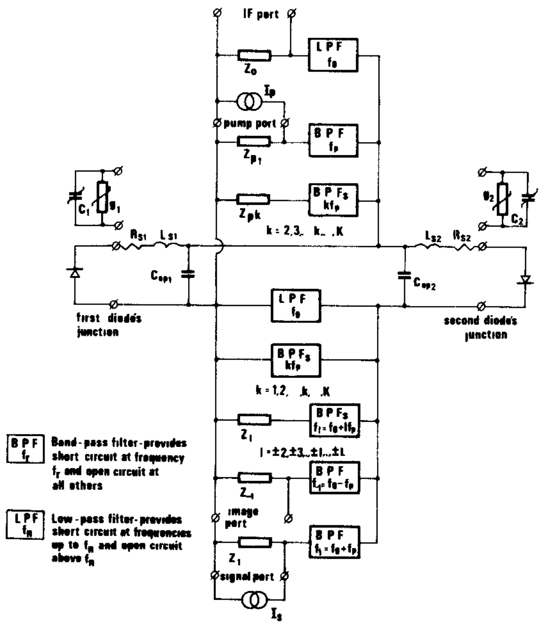

Fig. 9. Crossbar mixer model used in the analysis.

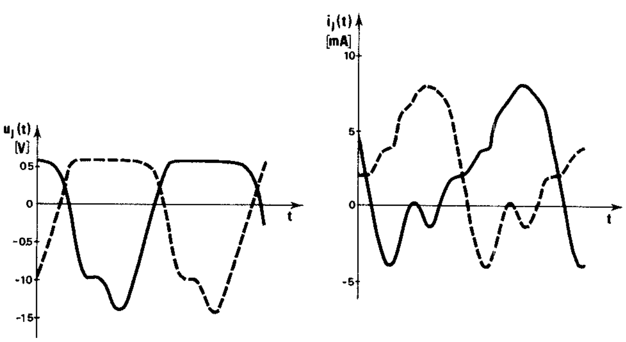

Fig. 10. Crossbar mixer: voltage and current waveforms at diodes' junctions ($I_o = 2.4$ mA).

V. Crossbar Mixer Example

A schematic diagram of the crossbar mixer is shown in Fig. 8. In this mixer configuration a pair of diodes in connected in series across the broadwalls of the signal waveguide. A metal crossbar serves as a mechanical support for the diodes and as a transmission line for the incoming LO pumping signal and the IF output signal. The diodes are electrically in parallel with respect to the transmission line formed by the crossbar and in series with respect to the waveguide. The diodes therefore can simultaneously match the relatively high impedance of the waveguide and the relatively low impedance of the transmission line without impedance transformers. The diodes are driven out of phase by the pump which leads to balanced mixer properties. Encouraging performance of the crossbar mixer configuration has been confirmed [13], [14], and this type of mixer is commercially available [15].

The mixer model used in the analysis is given in Fig. 9. The Schottky-barrier diodes are characterized by

$$i_g = I_s\left[\exp(qu_j/\eta kT) - 1\right]$$

$$c = C_o(1 - u_j/\Phi)^{-\gamma}$$

and the series resistances R_s. In the example the GaAs diodes' parameters are $R_s = 5\ \Omega$, $C_o = 9.5$ fF, $\eta = 1.1$, $\Phi = 0.9$ V, $\gamma = 0.5$, $I_s = 12.7 \cdot 10^{-12}$ A. Whiskers' inductances

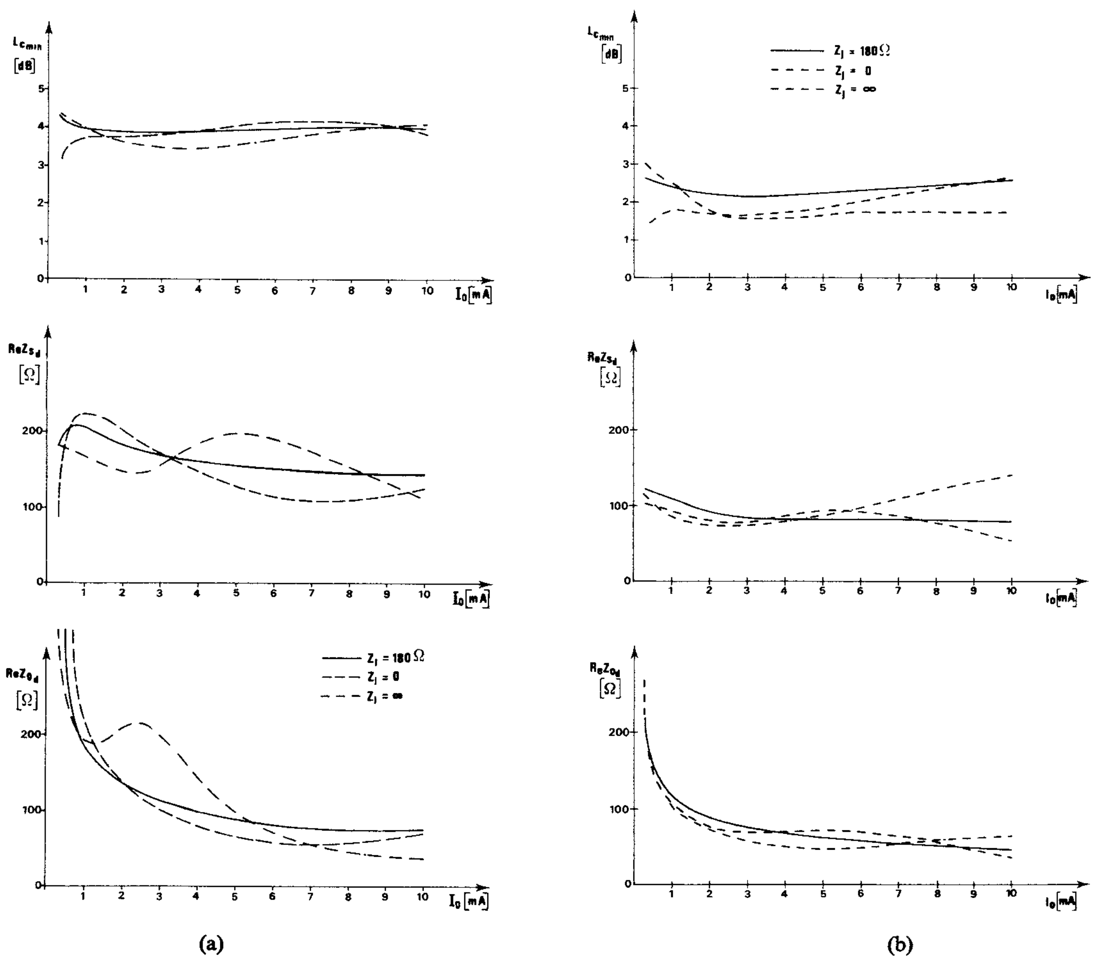

Fig. 11. Crossbar mixer: lowest achieveable conversion losses $L_{C_{\min}}$ and matching signal Re Z_{s_d} and IF Re Z_{0_d} resistances versus rectified currents I_o. (a) Image impedance Z_i equal to signal impedance Z_s. (b) Image opencircuited $Z_i=\infty$.

and parasitic capacitances are 0.2 nH and 7.5 fF, respectively. Six pump harmonics and six small-signal sideband components ($L=6$) were considered in the analysis. Some of the results computed for Q-band (36-GHz signal and 750-MHz IF frequencies) mixer working at temperature $T=298$ K are presented in Figs. 10 and 11.

Comparing the results it can be noticed that short or open circuiting of the idle frequencies do not lead to distinct improvements in conversion losses if the image impedance Z_i is equal to the signal impedance Z_s. In this case 4-dB conversion losses are achieveable providing that Re $Z_s=180\ \Omega$ and Re $Z_0=120\ \Omega$. In image recovery mixers much better practical results can be obtained with open-circuited image rather than with shortcircuited. Open circuited image ($Z_i=\infty$) leads to an unconditionally stable low sensitive mixer with 2.2 dB lowest achieveable losses. Conversion losses can be further decreased by means of reactive loads at the idle frequencies. It is more profitable to open circuit the idle frequencies. This gives $L_{C_{\min}}=1.6$ dB together with easier realizeable Z_s and Z_0. Open-circuits at the idle frequencies are better also in the case of short circuited image ($Z_i=0$). $L_{C_{\min}}=2.4$ dB are possible with easy realizeable Re $Z_s=210\ \Omega$ and Re $Z_0=50\ \Omega$. However such a mixer is sensitive to the pump and the reactance of the image impedance (Fig. 11(d)). It can be even potentially unstable. In this mixer case it is difficult to achieve low conversion losses due to high sensitivity to the signal and IF impedances.

VI. Summary and Conclusions

The theory given in the paper permits both the nonlinear and linear analyses of mixers with any number of diodes. In this theory, diodes are assumed to have both nonlinear conductance and capacitance. No restrictions are placed on the linear embedding network. It is only assumed that properties of the time-invariant part of the circuit are known at respective frequencies. It is not necessary to determine the equivalent circuit of the network. No simplifying assumptions other than those of most advanced one-diode mixer analyses are taken.

A computer program written in Fortran has been developed for practical application of this theory. The program has been thoroughly tested and its value in two-diode

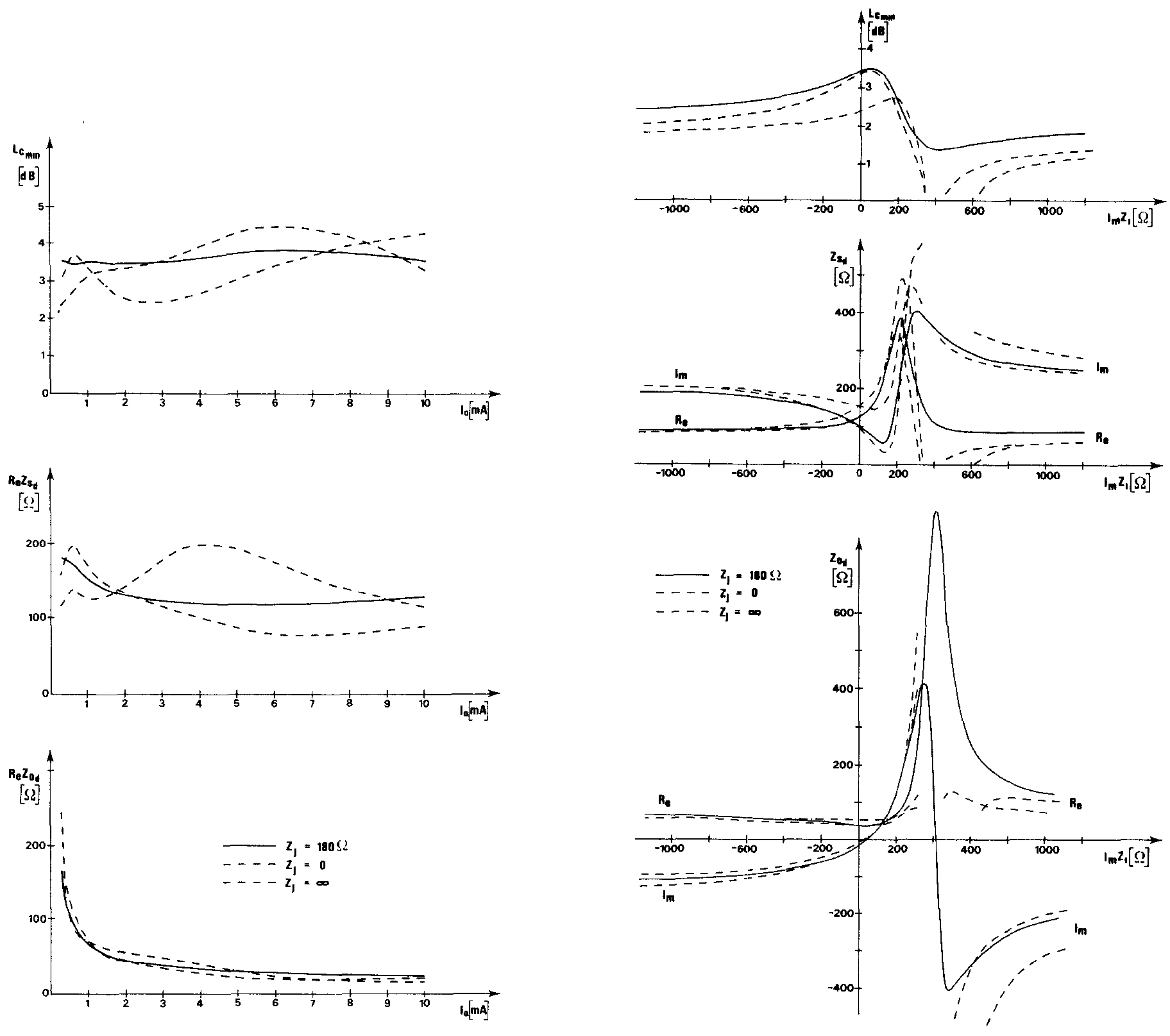

(c) (d)

Fig. 11. (c) Image shortcircuited $Z_i = 0$ (d) versus image reactance Im Z_i for Re $Z_i = 0$ and $I_o = 2.4$ mA. Z_j are external impedances at idle frequencies.

mixers analyses has been proved. In the paper, the cross-bar mixer example and some practical results of its analysis are provided to illustrate the theory.

The authors believe that the theory introduced here for mixer analyses may also be applied in analyzing other microwave circuits with diodes.

References

[1] H. C. Torrey and C. A. Whitmer, *Crystal Rectifiers*, (M.I.T. Radiation Lab. Series, vol. 15). New York: McGraw-Hill, 1948.

[2] A. A. M. Saleh, *Theory of Resistive Mixers*. Cambridge, MA: M.I.T. Press, 1971.

[3] M. R. Barber, "Noise figure and conversion loss of the Schottky barrier mixer diode," *IEEE Trans. Microwave Theory Tech.*, vol. MTT-15, pp. 629–635, Nov. 1967.

[4] S. Egami, "Nonlinear, linear analysis and computer aided design of resistive mixers," *IEEE Trans. Microwave Theory Tech.*, vol. MTT-22, pp. 270–275, Mar. 1974.

[5] W. K. Gwarek, "Nonlinear analysis of microwave mixers," M. S. thesis, M.I.T., Cambridge, MA, Sept. 1974.

[6] W. K. Gwarek, "Computer aided analysis of a one-diode microwave mixer," Ph.D. dissertation, Dep. Electron. Tech. Univ. Warsaw, Warsaw, Poland, 1977.

[7] A. R. Kerr, "A technique for determining the local oscillator waveforms in a microwave mixer," *IEEE Trans. Microwave Theory Tech.*, vol. MTT-23, pp. 828–831, Oct. 1975.

[8] D. N. Held, "Analysis of room temperature millimeter-wave mixers using GaAs Schottky barrier diodes," Sc.D. dissertation, *Dep. Elec. Eng., Columbia Univ.*, New York, NY., 1976.

[9] D. N. Held and A. R. Kerr, "Conversion loss and noise of microwave and millimeter-wave mixers: Part 1—Theory," and "Part 2—Experiment," *IEEE Trans. Microwave Theory Tech.*, vol. MTT-26, pp. 49–61, Feb. 1978.

[10] A. R. Kerr, "Noise and loss in balanced and subharmonically pumped mixers: Part I—Theory" and "Part II—Application," *IEEE Trans. Microwave Theory Tech.*, vol. MTT-27, pp. 938–950, Dec. 1979.

[11] M. T. Faber, "Linear analysis of a multidiode mixer" (in Polish), in *Proc. III National Conf. Circuit Theory Electronic Circuits*, (Stawiska, Poland), 1979, pp. 369–378.

[12] R. Q. Twiss, "Nyquist's and Thevenin's theorems generalized for nonreciprocal linear networks," *J. Appl. Phys.*, vol. 26, no. 5, pp. 599–602, May 1955.

[13] G. B. Stracca, F. Aspesi, and T. D'Arcangelo, "Low-noise microwave down-converter with optimum matching at idle frequencies," *IEEE Trans. Microwave Theory Tech.*, vol. MTT-21, pp. 544–547, August 1973.

[14] L. T. Yuan, "Design and performance analysis of an octave bandwidth waveguide mixer," *IEEE Trans. Microwave Theory Tech.*, vol. MTT-25, pp. 1048–1054, Dec. 1977.

[15] Data Sheet, SpaceKom Mixers (Strip-Guide Mixers).